An Inkjet-Printed Capacitive Sensor for Ultra-Low-Power Proximity and Vibration Detection

Steven D. Gardner, Muklasur R. Opu, Mohammad R. Haider
School of Engineering, University of Alabama at Birmingham, Birmingham, AL, USA
{stevendg, mopu, mrhaider}@uab.edu

***Abstract*—The field of inkjet-printed circuits and sensors has yet to reach commercial maturity but is showing significant success in research with ultra-low power, paper-thin, flexible and biodegradable devices that are magnitudes less expensive to fabricate than silicon-based circuits. One such implementation, as discussed in this work, is with capacitive-based sensors, where charge fluctuations in and around the plates' gap region alter the output current signal. The resulting functionalities are vibration/proximity sensing, where the magnitude of the output current reflects the environmental perturbations. The power efficiency, flexibility, and cost effectiveness of the sensor as reported in this work demonstrates that simple fabrication with inkjet-printing can form green-friendly, high-functioning devices as alternatives to standard silicon-based approaches. Silver nanoparticle ink was inkjet-printed onto a PET film substrate with the design of two parallel plates with a narrow gap region between them that is cut and filled with hexagonal boron nitride nanoparticle ink, which is a dielectric and charge trapping material. Fringe-field capacitance emanating from the flat substrate around the gap region of the parallel plates fluctuates according to the vibration and proximity of environmental interference. The sensor operates at an average of 4.9 nano-Watts with a 3.3V supply, senses floor/table vibrations from 5 feet away, costs $0.19 to fabricate, and is compatible with additive manufacturing for high-volume printing. Applications include: movement detection near irregularly shaped surfaces; touch-less interfaces for initiating devices; traffic monitoring and prediction with post-processing algorithms; and high-volume deployment for large-area vibration observations.**

***Index Terms*—inkjet-printed devices, proximity sensor, flexible circuits, additive manufacturing**

I. Introduction

The growth in markets for vibration and proximity sensors is expected to be driven by the increasing demand for smart, Internet of Things (IoT)-connected devices, and automation[1]. For instance, the increasing importance of safety is leading to non-contact sensors such as the capacitance proximity sensor of this work [2]. The growth of IoT devices makes application to smart systems for real-time monitoring and control of large systems more viable with less human interaction. Additionally, these types of sensors are being merged with artificial intelligence and machine learning algorithms for monitoring, classification, and prediction of multi-faceted signals [3]. The trend towards miniaturization is seen across all technology for smaller, more efficient, and green-friendly sensors that can be worn or applied in high volumes. Finally, the automotive, military, and environmental industries are driving demand for these sensors with safety systems, on-drone deployment, large-area monitoring, etc. Common types of proximity or vibration sensors currently on the market and being researched are outlined in Table I [4]. Limitations of existing silicon-based proximity and vibration sensors are high costs, hazardous waste production from fabrication, and digital security . This work benefits (1) environmental friendliness by avoiding production of hazardous waste, (2) reduced cost by using commercially available components and a simple fabrication process, and (3) digital security friendliness since it is an edge device, only connecting to the cloud when the sensor reaches a threshold to initiate a process.

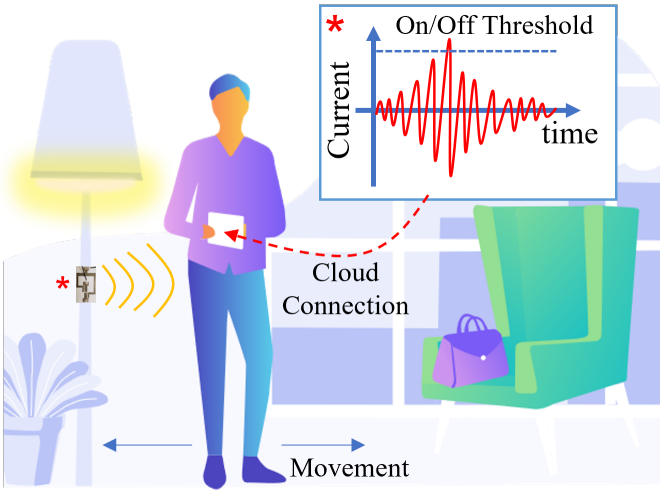

Fig. 1: Concept diagram of the inkjet-printed fringe field capacitance sensor within the potential application of smart homes where the data is cloud-connected for fast feedback.

Figure 1 shows an application example of the inkjet-printed sensor of this work in the context of smart homes. Walking past or waving a hand over the sensor can initiate the lights, TV, or anything IoT connected, and can be placed on any surface or worn. The sensor is a cost effective, low-profile, and low-power device. The contents of this work are as follows. First, inkjet-printed technology is introduced (Section II) and the fringe-field capacitance (FFC) sensor working principles are explained in Section III, followed by an explanation of the device fabrication in Section IV. The testing conditions and methods are defined in Section V and the results are shown and discussed in Sections VI and VII, respectively. Lastly, a conclusion with future planned research is elaborated in Section VIII.

TABLE I: Various Types of Common Proximity Sensors

Sensor Type	Description
Capacitive Proximity Sensors	Senses changing capacitance.
Inductive Proximity Sensors	Senses changing inductance, includes RFID-based sensors.
Photoelectric Sensors	Senses changing photonic (light) exposure.
Ultrasonic Sensors	Senses high-frequency sound waves.
Magnetic Proximity Sensors	Senses changing magnetic fields.
Piezoelectric Sensors	Senses changes in mechanical strain.
Hall-effect Sensors	Uses the Hall effect to detect magnetic fields.

II. Inkjet-Printed Technology

Inkjet printed (IJP) technology takes advantage of piezoelectric printer dynamics to eject uniquely behaving nano-particles from its print head onto a substrate. This growing field of circuit creation has allowed for flexible, biodegradable, repeatable, highly inexpensive, and fast circuit/sensor fabrication, with a plethora of sensing applications that vary according to material choice and circuit structure [5]. The basic IJP process follows the steps as seen in Fig. 2. Nano-particle inks are first filled into refillable cartridges and placed in the inkjet printer. The substrate is then chosen which may be treated prior to printing for improved ink adhesion. Some treated substrates are commercially available, as is chosen for this work (see Section IV). The print patterns are designed on any digital editing program and then the pattern is printed layer-by-layer. Between layers, the substrate may be thermally cured for continuous bulk formation of the nano-particles. Prior works published using inkjet printing to form sensors that follow the simplified fabrication process have been conducted for a variety of applications, some shown in the references [6]–[8]. The fabrication process varies in research settings to include involved and expensive processes/equipment such as plasma and gas treatment, non-IJP ink deposition, spin-coating, magnetron sputtering, slot-die coding, precise parameter control, usage of novel materials, and many other custom techniques [9].

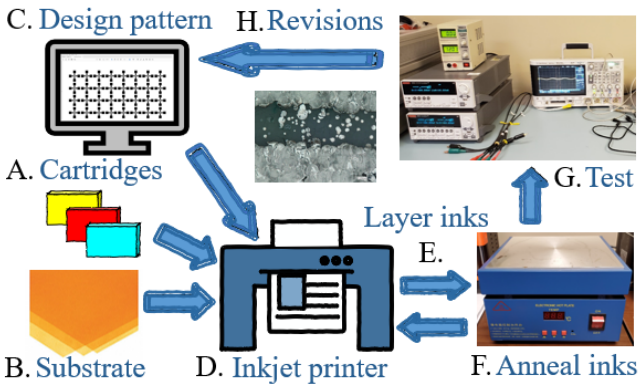

Fig. 2: Generic fabrication process using the IJP setup.

III. FFC Sensor Working Principles

The equivalent capacitive circuit for two parallel silver plates inkjet printed onto a substrate is shown in Fig. 3. The capacitance formed between these two parallel printed lines can be represented by the famous Palmer's equation. The total capacitance manifests a constant lateral capacitance, C_l, and a fringe capacitance, C_f. The charge, Q, stored across the capacitor due to the constant DC voltage, V, is defined as

$$Q = C \times V = (C_l + C_f) \times V \tag{1}$$

The C_f varies due to the presence of dieletric material of the feet and creates a dynamic current flow to balance the charge equation.

$$i = \frac{dQ}{dt} = V \times \frac{dC_f}{dt} \tag{2}$$

An electromagnetic field (EMF) is generated by the applied voltage in the capacitor model. However, the IJP capacitor's EMF lies beyond the substrate plane, making its capacitance vary based on how the EMF is perturbed by physical interference. The low voltage supply and current output of the IJP sensor causes the EMF of the IJP capacitor to be small, minimizing the unwanted interference.

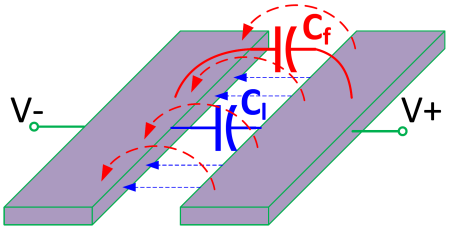

Fig. 3: IJP capacitor working principle. The IJP capacitor emits a small EMF that changes the charge when touched, bent, or deformed.

IV. Inkjet-Printed FFC Fabrication

Fabrication of he sensor was done in the BioIntegrated Circuits (BIC) laboratory at UAB. As depicted in Fig. 4, the IJP FFC sensor is designed as silver (Ag) nanoparticle parallel plates printed onto polyethylene terephthalate (PET) film with a standard drop-on-demand, piezoelectric printer (Epson XP-960). The silver parallel plates are printed with a gap of approximately 0.5 mm, chosen to be above the printer's rated minimum resolution of 0.3 mm to prevent channel shorting via ink splattering. The ink is then annealed by placing the sensor on a hot plate at 60°C for 5 minutes. Hexagonal Boron Nitride (hBN) is a dielectric and charge trapping material that was deposited as an ink onto the channel (gap) region of the terminals. After drying the ink by curing on a hotplate again at 60°C for 5 minutes, a small cut is made with a blade on the hBN along the gap to increase the charge trapping abilities and thus magnify the sensing behavior. Two terminals of the four shown in Fig. 4 are not used in this work, but were included in the design to allow more variations of testing that are outside the scope of this work but will be

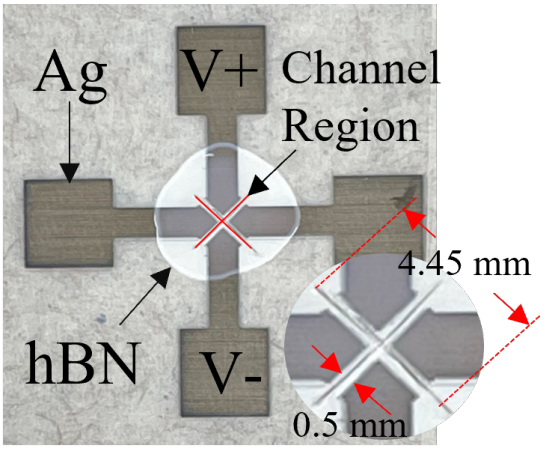

Fig. 4: IJP FFC Sensor shows the different materials used to fabricate the design, and a red line along the gap region showing where a cut was made, defining the gap length.

used in future research. Another similar design not shown in this work was also fabricated, where the gap length is significantly longer to understand more about how the channel length effects the fringe field intensity.

The samples printed for this work have a substrate thickness of 135 μm and costs \$180 (NB-TP-3GU100 Mitsubishi Paper Mills) for 100 sheets (\$1.80/sheet or \$0.09/sample at 20 samples per page). The cost to print is estimated from a 100 mL bottle of silver nanoparticle ink costing \$120 (NBSIJ-MU01 Mitsubishi Paper Mills) at 220 pages per 11 mL cartridge (\$0.0027/sample), and 5 mL bottle of hBN ink (Sigma Aldrich 901410-5ML) costing \$225 (\$0.102/sensor). The total estimated cost for each sensor is \$0.19 per sample. Comparatively, capacitive proximity sensors cost anywhere from \$8 for low-quality sensors to over \$300 for high-precision sensors, and their fabrication creates hazardous waste byproducts and is not additive or flexible.

V. Testing Parameters and Conditions

The testing procedures were performed in the BIC lab and are as follows. Vibration sensitivity was tested by walking from the furthest distance the FCC sensor could detect incrementally 1 foot at a time toward the sensor and then walking back in the same manner, all while collecting its output current signal. This was repeated several times for 4 samples at different supply voltages including [1.2, 2.25, 3.3, 5, 9, 10] V. The voltages chosen are based on typical voltage supply ranges for modern electronics, with the intent being eventual integration with microcontrollers and ASICs. The proximity tests were performed by waving a hand over the sensor starting from the furthest detectable distance, gradually moving the waving hand closer to the sensor. This test was repeated similarly to the vibration test over the same 4 samples. Data was collected at 60 Hz with a Keithley 2604B SourceMeter through their supported program called KickStart. The data was post-processed in Excel for analysis and plot generation.

VI. Testing Results

Two different designs were tested, the first being the sensor shown in Fig. 4, and the second being one not shown in this work. However, a generalization can be made about the FFC sensor from the second design, which featured the same gap width but longer gap length. Comparing the testing results of both designs shows that the gap length influences the sensitivity of the FFC sensor, with longer gap lengths resulting in greater charge trapping and therefore higher fringe-field capacitance. Thus, the longer the gap length, the greater the sensitivity and lower supply power needed to operate. The ratio of gap width to gap length is a finite way track relative sensitivity between the different designs. For the FFC sensor of Fig. 4, the width:length ratio is 1:9 and for the sensor not shown it is 1:19.

The hand waving test as described in Section IV was performed on both sensors, and the sensor not shown had the results of Fig. 5. Starting from the furthest detectable distance (18 inches) the hand was moved closer to the sensor from above while waving the hand until 4 inches away from the sensor, and then moved back away in the same manner to the start point. The amplitude of the current signal increases non-linearly as the hand moves to and from it linearly, indicating that the fringe-field capacitance is a non-linearly shaped field, as expected from the working principles of Section III. The average current output was 782 pA at 10V for an average power of 7.8 nW. Applying lower voltages cause the current output to also be lower, making the average power significantly decrease.

The walking test was performed on both the sensor designs, and the test results of the Fig. 4 design is shown in Fig. 6. There, three voltages commonly seen in electronics were used

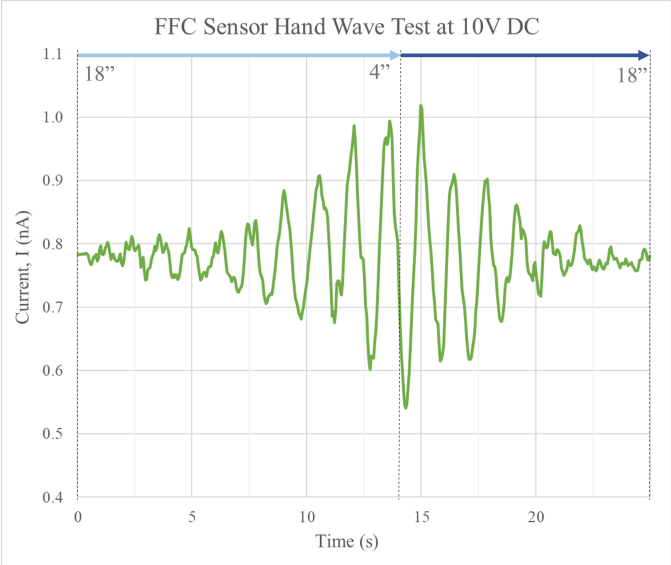

Fig. 5: The current output according to the hand waving tests is shown. The amplitude of the current signal increases non-linearly as the hand gets closer to the sensor, and vice versa when moving the hand away.

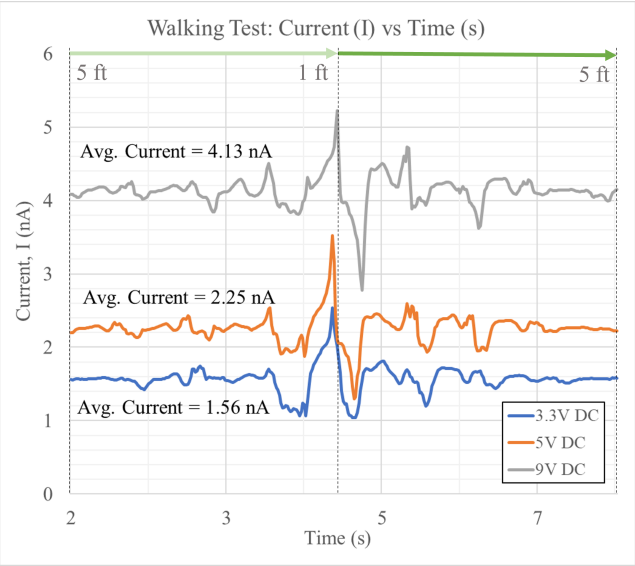

Fig. 6: Results from the vibration test are shown for three applied voltages. Walking towards and away from the sensor shows non-linearly increasing current amplitude.

to see the changes in signal biasing and behavior. It is clear that higher supply voltages correspond to higher biasing of the signal, but the behavior stays consistent. As vibrations translate through the floor and table by foot steps, the signal shows a proportional amplitude response as it continuously works to balance the charge equations of Section III. Average power for [3.3, 5, 9] V are [4.9, 11.3, 37.4] nW, respectively. The power increase is non-linear and thus power consumption increases as voltage supply is increased, reaching a saturation point where any higher voltages does not change power consumption but causes the sensor to degrade in sensing capabilities. Tests were performed below 3.3 V but the interference at such low current values (i.e., low pA range) causes the signals to have no distinction. Thus, 3.3V is the minimum suggested supply voltage for the FFC sensor.

VII. Discussion and Future Work

Fabrication of the FFC sensors has points of inconsistency depending on the volume of hBN applied, the curing distribution, and quality of the cut channel region. Human error causes subtle variation in the biasing of the sensors, although the sensing behavior is consistent across all tests. The concentration of the hBN ink drop, which can vary from 1-2 μL, causes current averages to slightly vary between samples due to the resulting ink thickness after curing. Curing also suffers from the ring effect where the edges contain higher concentrations of the nanoparticles which can be seen in Fig. 4. The quality of the channel region cut depends on the blade sharpness and cut depth control, effectively defining the cut's width and length. Larger area cuts alter the capacitor's fringe-field which is a factor to defining its sensitivity. Streamlining the fabrication process by automating application of the hBN and channel region cut will result in more consistent sensor biasing.

The channel width to length ratio defines the FFC's relative sensitivity and can be adjusted easily for optimized power utilization. Compatibility with microcontroller is possible due to the applied voltage and minimal power utilization. However, output signal boosting may be necessary for analog to digital conversion. A study on the longevity and durability is considered in future work, along with integration with microcontrollers and proof-of-concept devices within an IoT framework.

VIII. Conclusion

An inkjet-printed and low-fabrication sensor was made that forms a fringe-field capacitance around its channel region when voltage is applied, causing current signal fluctuations with environmental perturbations. This fringe-field capacitor sensor was tested for its sensitivity to vibration by walking toward and away from it, along with waving the hand above it at different distances. The results show that the current signal works to balance its charge equation according to the intensity that the fringe-field capacitance fluctuates. This low-cost and flexible sensor may be used in many applications from large scale deployment to personalized wearable sensing in environmental studies, military tracking, safety technology, and smart home settings.

IX. Acknowledgment

This research was partially supported by National Science Foundation (Award Nos. ECCS-1813949 and ECCS-2201447). However, any opinions, findings, conclusions, or recommendations expressed herein are those of the authors and do not necessarily reflect the views of the funding agencies.

References

[1] M. Javaid, A. Haleem, S. Rab, R. Pratap Singh, and R. Suman, "Sensors for daily life: A review," *Sensors International*, vol. 2, p. 100121, 2021.

[2] J. Liang, J. Wu, H. Huang, W. Xu, B. Li, and F. Xi, "Soft sensitive skin for safety control of a nursing robot using proximity and tactile sensors," *IEEE Sensors Journal*, vol. 20, no. 7, pp. 3822–3830, 2020.

[3] F. Xia, F. Campi, and B. Bahreyni, "Tri-mode capacitive proximity detection towards improved safety in industrial robotics," *IEEE Sensors Journal*, vol. 18, no. 12, pp. 5058–5066, 2018.

[4] R. Moheimani, P. Hosseini, S. Mohammadi, and H. Dalir, "Recent advances on capacitive proximity sensors: From design and materials to creative applications," *Journal of Carbon Research*, vol. 8, no. 2, p. 26, 2022. [Online]. Available: https://www.mdpi.com/2311-5629/8/2/26

[5] M. A. Shah, D.-G. Lee, B.-Y. Lee, and S. Hur, "Classifications and applications of inkjet printing technology: A review," *IEEE Access*, vol. 9, pp. 140 079–140 102, 2021.

[6] R. Lu, M. R. Haider, S. Gardner, J. I. D. Alexander, and Y. Massoud, "A paper-based inkjet-printed graphene sensor for breathing-flow monitoring," *IEEE Sensors Letters*, vol. 3, no. 2, pp. 1–4, 2019.

[7] S. Gardner, M. R. Haider, M. T. Islam, J. I. D. Alexander, and Y. Massoud, "Aluminum-doped zinc oxide (zno) inkjet-printed piezoelectric array for pressure gradient mapping," *62nd IEEE International Midwest Symposium on Circuits and Systems*, 2019.

[8] S. Gardner, J. I. D. Alexander, Y. Massoud, and M. R. Haider, "An inkjet-printed paper-based flexible sensor for pressure mapping applications," *IEEE International Symposium on Circuits and Systems (ISCAS)*, 2020.

[9] H. Matsui, Y. Takeda, and S. Tokito, "Flexible and printed organic transistors: From materials to integrated circuits," *Organic Electronics*, vol. 75, 2019.